Author/s:
Shirbin, SJ;Insua, I;Holden, JA;Lenzo, JC;Reynolds, EC;O'Brien-Simpson, NM;Qiao, GG

Title:
Architectural Effects of Star-Shaped “Structurally Nanoengineered Antimicrobial Peptide Polymers” (SNAPPs) on Their Biological Activity

Date:
2018-11-07

Citation:
Shirbin, S. J., Insua, I., Holden, J. A., Lenzo, J. C., Reynolds, E. C., O'Brien-Simpson, N. M. & Qiao, G. G. (2018). Architectural Effects of Star-Shaped “Structurally Nanoengineered Antimicrobial Peptide Polymers” (SNAPPs) on Their Biological Activity. Advanced Healthcare Materials, 7 (21), https://doi.org/10.1002/adhm.201800627.

Persistent Link:
https://hdl.handle.net/11343/284413

DOI: 10.1002/ ((please add manuscript number))

**Article type: Full paper**

# Architectural Effects of Star-Shaped 'Structurally Nanoengineered Antimicrobial Peptide Polymers' (SNAPPs) on their Biological Activity

*Steven J. Shirbin,[‡] Ignacio Insua,[‡] James A. Holden, Jason C. Lenzo, Eric. C Reynolds, Neil M. O'Brien-Simpson* and Greg G. Qiao**

Dr. S. J. Shirbin, Dr. I. Insua, Prof. G. Qiao

Polymer Science Group

Department of Chemical & Biomolecular Engineering

University of Melbourne

Parkville, VIC 3010, Australia

E-mail: gregghq@unimelb.edu.au

Dr. I. Insua, Dr. J. A. Holden, Dr. J. C. Lenzo, Prof. E. C. Reynolds, Prof. N. M. O'Brien-Simpson
Melbourne Dental School and the Bio21 Institute of Molecular Science and Biotechnology Oral Health CRC, University of Melbourne

Parkville, VIC 3010, Australia

E-mail: neil.obs@unimelb.edu.au

Keywords: SNAPP, antimicrobial, star polymer, architecture, polypeptide

In this work, we investigate the effect of two key structural parameters of star-shaped SNAPPs "Structurally Nanoengineered Antimicrobial Peptide Polymers" on their antimicrobial activity and biocompatibility: number of arms and arm length. A library of star-shaped SNAPPs is prepared, containing varying arm numbers and arm lengths. Antimicrobial assays are then performed to assess the capacity of the SNAPPs to disrupt the membrane, inhibit the growth and kill pathogenic bacteria. A major finding of the study is that increasing arm number and length of SNAPPs enhanced antimicrobial activity, which can be respectively attributed to the higher local concentrations of polypeptide arms and increased α-helical content. SNAPP architecture was shown to affect the bacteria membrane state and therefore mechanism of killing. Two more potent structures with up to twice the antimicrobial activity of our previously reported SNAPP are discovered in this process. Toxicities of the SNAPPs also increased with arm number and arm length, however therapeutic index calculations identified a 16-arm SNAPP and an easier to prepare 4-arm SNAPP as the best therapeutic agents. The biocompatibility of the SNAPP with the best biological activity is also evaluated *in vivo*, showing no markers of systemic damage in mice.

## 1. Introduction

The world is currently experiencing an era where large numbers of pathogenic microbes are becoming resistant to conventional medications whilst faced with limited effective antimicrobial options.[1-3] According to the World Health Organisation (WHO), even those antimicrobial agents in

the current development pipeline are still insufficient to mitigate the threat of antimicrobial resistance, due to the lack of new antimicrobial classes and new targets/modes of action.[3] Hence, the hunt for new alternative treatments has become a matter of urgency.[4] Amongst the alternative antimicrobial therapies currently under development,[5] synthetic mimics of antimicrobial peptides (AMPs) are becoming increasingly more promising. Synthetic mimics of AMPs often display the high activity, broad-spectra, and low propensity for resistance common to natural AMPs,[6, 7] whilst overcoming the cytotoxicity and biostability limitations affecting their natural counterparts.[6, 8, 9] Recently, we reported on the preparation of a new class of synthetic AMP mimics, termed 'Structurally Nanoengineered Antimicrobial Peptide Polymers' or "*SNAPPs*", in the form of star-shaped polypeptide nanoparticles containing cationic lysine and hydrophobic valine amino acid residues.[10] These SNAPPs demonstrated excellent antimicrobial properties, with sub-μM activity against a range of Gram-negative bacteria and some of their concerning multidrug resistant (MDR) strains. The SNAPPs demonstrated to be the first synthetic antimicrobial polymer with *in vivo* efficacy against colistin-resistant and MDR gram-negative pathogens.[10] Importantly, these SNAPPs demonstrated low toxicity towards mammalian cells and no bacterial resistance to the SNAPPs was detected.

Comparisons between linear and star-shaped SNAPPs were performed in the above study, proving the superior antimicrobial activity of the latter.[10] This result demonstrated that polymer architecture determines the antimicrobial activity of polypeptides. However, structural parameters within the star polymer itself were not comprehensively investigated, such as the effect of polypeptide arm number and/or polypeptide arm length (i.e. degree of polymerization, DP). To date,

the structural effects of synthetic polypeptide AMP mimics on antimicrobial activity have only been seen in linear [11-13] or graft polymer [14, 15] systems, with DP being the only structural determinant assessed. A systematic investigation into the architectural effects of star-shaped SNAPPs is necessary to understand the structure-activity relationships of star-shaped antimicrobial polypeptides, and thus guide the development of new star SNAPPs with improved biological properties.

In this work, we investigate the effect of two key structural parameters of star-shaped SNAPPs, number of arms and arm length (*i.e*. DP), on their antimicrobial activity and biocompatibility. A small library of star-shaped SNAPPs was prepared, containing varying arm numbers and arm lengths. *Escherichia coli* was used as a model bacterium to screen their antimicrobial activity. Antimicrobial assays were performed to assess the capacity of the SNAPPs to disrupt the membrane, inhibit the growth and kill pathogenic bacteria. Our results showed overall enhanced antimicrobial activities for SNAPPs bearing more and longer polypeptide arms, which could be respectively attributed to the higher local concentrations of polypeptide arms and increased α-helical conformation – a common property to the mechanism and activity of many natural AMPs. New SNAPPs with up to twice the antimicrobial activity of our previously reported SNAPP were discovered in this process. Overall, the toxicity of SNAPPs also increased with arm number and arm length. Therapeutic index calculation identified a new easier-to-prepare star SNAPP architecture with a similar therapeutic index to the highest found in this collection. The biocompatibility of the SNAPP with the best biological activity discovered thus far was also evaluated *in vivo*, with no indication of systemic toxicity.

## 2. Results and Discussion



### 2.1 Design, synthesis and characterisation of SNAPPs

To test the effect of these two parameters of arm number and arm length, a library of SNAPPs containing a variation of arm number and arm lengths were sought for this study. We prepared SNAPPs through our previously reported method involving the random ring opening polymerisation (ROP) of cationic capable L-lysine (*Ɛ*-carboxybenzyl/CBz/Z-protected) and hydrophobic racemic D,L-valine amino acid *N*-carboxyanhydride (NCA) monomers.[10] Polymerisation was performed through a core-first approach, initiated by the terminal primary amines of a poly(amido amine) (PAMAM) dendrimer core. The reaction was conducted in ice, as opposed to the previously reported method at room temperature, to reduce the chances of chain-termination side reactions and improve polymerisation control.[16, 17]

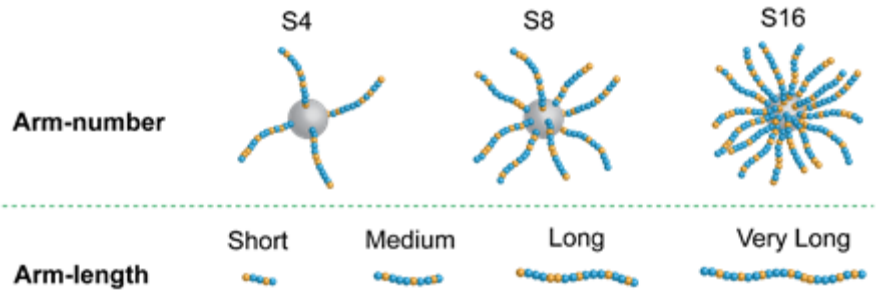


**Figure 1**. Arm number and arm length of star-shaped SNAPPs are investigated in this study.

Under this protocol, we prepared a library of cationic lysine and hydrophobic valine star-shaped SNAPPs in the form of 4-arm (S4), 8-arm (S8) and 16-arm (S16) stars. Stars of varying arm length were also prepared (**Figure 1**). Using the core-first approach, NCA monomers were polymerised randomly by primary amine initiation from a PAMAM core in ice (~ 4ºC). Variation in arm number was achieved through use of different PAMAM dendrimer generations with a defined number of peripheral primary amine initiation sites. The resulting CBz/Z-protected lysine residues were then deprotected with hydrobromic acid, generating fully water-soluble polymers (**Scheme 1**).

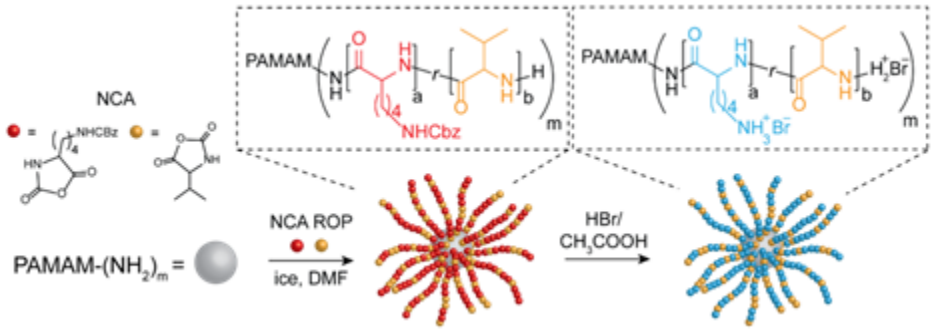


**Scheme 1**. Synthesis of lysine and valine SNAPPs in ice through NCA ROP of lysine and valine *N*-carboxyanhydride (NCA) monomers by initiation from the terminal amines of poly(amido amine) (PAMAM) dendrimers. Generation 0, 1 and 2 PAMAM dendrimers with 4, 8 and 16 peripheral primary amines respectively (**Figure S2**) were used to prepare S4 (*m*=4), S8 (*m*=8) and S16 (*m*=16) star shaped SNAPPs. Deprotection of lysine CBz/Z group with HBr yielded fully water-soluble star SNAPPs.

In line with our previous studies, we selected a theoretical lysine-to-valine ratio of approximately 2.5:1. This ratio represents a hydrophobic (valine) molar fraction within the 20-40% range, commonly observed to be most effective for antimicrobial polymers,[18-20] while also promoting full water solubility. All prepared star-shaped SNAPPs and their corresponding characterisation data is shown in **Table 1**. All stars contained similar lysine to valine ratios close to the theoretical ratio of 2.5:1, as determined through $^{1}$H NMR analysis (see example in **Figure S3**). Absolute molecular weight (MW) of the stars was calculated through size exclusion chromatography (SEC) using light scattering measurements, which in conjunction with NMR studies, led to accurate determination of star arm length (arm DP) and arm composition.

**Table 1**. Characterisation of SNAPPs.

| SNAPP code[a)] | Arm number | Lys/Val[b)] | $M_n$ (kDa)[c)] | $Đ$[c)] | Arm DP | $D_H$ (nm)[d)] |
|---|---|---|---|---|---|---|
| $S16_M$ | 16 | 2.4 | 41.1 | 1.7 | 14 | 9.6 ± 0.5 |
| $S16_L$ | 16 | 2.2 | 52.6 | 1.7 | 18 | 10.1 ± 0.5 |
| $S8_M$ | 8 | 2.4 | 23.4 | 1.5 | 16 | 7.3 ± 1.1 |
| $S8_{VL}$ | 8 | 2.6 | 43.4 | 1.8 | 29 | 12.4 ± 0.4 |
| $S4_S$ | 4 | 2.1 | 3.3 | 1.3 | 5 | 2.6 ± 0.1 |
| $S4_M$ | 4 | 2.3 | 8.8 | 1.3 | 12 | 4.0 ± 0.3 |
| $S4_L$ | 4 | 2.5 | 14.1 | 1.5 | 19 | 5.1 ± 0.5 |
| $S4_{VL}$ | 4 | 2.9 | 19.2 | 1.7 | 26 | 6.1 ± 0.3 |
| | | | | | | |

[a)] Numbers in SNAPP code represent star arm number, with subscript letters representing star arm length (*i.e.* arm DP): S = small, M = medium, L = long, VL = very long. [b)] Determined through $^1$H NMR analysis in $D_2O$. [c)] Absolute number-average molecular weight ($M_n$) and polydispersities ($Đ$) determined through SEC light scattering using measured dn/dc values. [d)] Hydrodynamic diameters ($D_H$) ± standard deviations determined by DLS. Values represent mean size-number values averaged from 3 measurements, each containing 15 runs.

The polydispersities of the SNAPPs ranged from 1.3-1.8 and were considerably lower than the SNAPPs reported previously.[10] It must be noted that the polydispersities of these particular star-shaped polypeptides are expected to be slightly higher than other polypeptide star systems in the literature[21, 22] due to the use of valine, an amino acid well known to produce insoluble β-sheet structures *in situ*, and therefore likely to have an impact on polymerisation control.[23-26] In fact, earlier attempts to prepare a 16-arm SNAPP with a higher valine content (lys/val ratio of 1.3) with similar arm DP, resulted in a significant increase in polydispersity (**Figure S1**). Despite this, the SEC profiles of all SNAPPs tested in this study displayed typical mono-modal profiles (see **Supporting Information**), with any SNAPPs showing bi or multi-modal spectra excluded from this study.

$S4_M$, $S8_M$ and $S16_M$ star shaped SNAPPs, each containing a similar medium (M) range arm length of *ca.* 14 repeat units per arm, were designed to investigate the effect of arm number on star performance (**Table 1**). This arm length was targeted as it was similar to the calculated arm length of the S16 SNAPP we reported previously.[10] As expected, SEC analysis showed an increase in star MW

with increasing arm number (**Table 1, Figure S4**). Due to the increase in PAMAM core size with generation/arm number,[27, 28] the hydrodynamic diameter of the stars was expected to slightly increase with arm number and this was indeed observed through dynamic light scattering (DLS) (**Table 1, Figure S9A**).

S4 stars were chosen as the platform to investigate the effect of SNAPP arm length due to their higher conversion efficiencies and lower polydispersities as expected when polymerising from the less sterically hindered 4-arm core. Four different arm lengths of the S4 SNAPP were investigated in this study with DP values of *ca*. 5 (short, S); 12 (medium, M), 19 (long, L) and 26 (very long, VL) (**Table 1**). SEC analysis and DLS respectively confirmed the increasing MW's (**Table 1, Figure S5**) and slightly increased hydrodynamic diameters (**Table 1, Figure S9B**) following increases in these S4 arm lengths.

In addition, the surface charge of the SNAPPs was assessed by zeta potential measurements, with similar values (36.8 ± 4.7 mV, mean ± SD) obtained across the SNAPP library (see **Figure S11**). This could be expected as the same relative lysine (cationic) and valine (hydrophobic) is present across the SNAPPs. As well, any increase in arm number and arm length of the SNAPPs is also accompanied by an increase in SNAPP size (see **Table 1**), therefore surface charge densities and zeta potential measurements can be expected to be relatively constant across the SNAPP library.

2.2 *In vitro* antimicrobial evaluation of SNAPPs

The antimicrobial activity of the SNAPPs presented in **Table 1** was evaluated *via* three distinct and complimentary assays (**Table 2, Figure S12**): i) Minimum membrane Disruptive Concentrations (MDCs) report on the capacity of antimicrobial materials to disrupt the inner/cytoplasmic membrane of bacteria.[29] In this assay, all bacteria are fluorescently labelled with the membrane-permeable probe Syto®9, whereas only bacteria with damaged/permeabilized membranes are labelled with the membrane-impermeable dye propidium iodide (PI). Thus, intact bacterial cells appear as Syto®9 positive events when measured by flow cytometry, while bacteria with damaged/permeabilized membranes show as double Syto®9-PI positive cells. ii) The Minimum Inhibitory Concentration (MIC) of SNAPPs was calculated by broth dilution, which is a standard antimicrobial assay that correlates the increase in turbidity of a culture with bacterial proliferation.[30] As such, the MIC indicates the lowest concentration of an antimicrobial agent that inhibits bacterial growth without necessarily killing the pathogen. iii) Finally, Minimum Bactericidal Concentrations (MBCs) were calculated by inoculation of mixtures of bacteria and SNAPPs on agar plates and subsequent counting of colony forming units (CFUs). Each CFU arises from the exponential growth of one individual bacterial cell, and as such, MBC provides a measurement of the dose required to kill bacteria inferred from the decrease in CFUs of bacterial cultures. In summary, all three assays (*i.e.* MDC, MIC and MBC) measure different antimicrobial effects, thus providing a broad understanding of the activity of SNAPPs against bacteria, and in all cases lower MDC/MIC/MBC values correspond to stronger antimicrobial activities. Assay outputs were analysed by, 1. molarity to compare activity on a molecule to molecule basis, thus changes in SNAPP antimicrobial activity can be ascribed to arm

number or arm length (change in MW) and, 2. Dose (μg/mL) of each SNAPP as this is a standard measurement in antibiotic literature and reporting activity in molarity and dose is recognised as best practice.[31]

Our initial studies focussed on the effect of the number of polypeptide arms of SNAPPs on their antimicrobial activity. To this end, the star polymers $S16_M$, $S8_M$ and $S4_M$ were tested against *E. coli*, which respectively contain 16, 8 and 4 polypeptide arms of very similar DP and amino acid composition (see **Table 1**). Both $S16_M$ and $S8_M$ displayed excellent antimicrobial activities against *E. coli*, as evidenced by their MDC, MIC and MBC values in the nM range (**Table 2**).

**Table 2**. Antimicrobial activity of SNAPPs against *E. coli* measured as minimum disruptive, inhibitory and bactericidal concentrations (*i.e.* MDC, MIC and MBC, respectively).

| SNAPP code | MDC [a] | | MIC [a] | | MBC [b] | | |
|---|---|---|---|---|---|---|---|
| | $\mu g \cdot mL^{-1}$ | nM | $\mu g \cdot mL^{-1}$ | nM | $\mu g \cdot mL^{-1}$ | nM | |
| $S16_M$ | 4.7 | 115 | 5.2 | 127 | 6.25 | 152 | |
| $S16_L$ | 3.3 | 62 | 4.4 | 85 | 3.12 | 59 | |
| $S8_M$ | 6.7 | 286 | 7.5 | 322 | 6.25 | 267 | |
| $S8_{VL}$ | 4.4 | 102 | 4.6 | 105 | 6.25 | 144 | |
| $S4_S$ | >100 | >30,000 | >100 | >30,000 | >100 | >30,000 | |
| $S4_M$ | 21.7 | 2,466 | 23.2 | 2,636 | 25 | 2,841 | |
| $S4_L$ | 6.4 | 455 | 7.9 | 560 | 12.5 | 887 | |
| $S4_{VL}$ | 7.9 | 412 | 7.7 | 403 | 12.5 | 651 | |
| | | | | | | | |

[a] MDC and MIC values were calculated by exponential regression of experimental data (**Supporting Information**). [b] MBC values calculated by CFU assay: standard deviation < 0.2 $\mu g \cdot mL^{-1}$ and $R^2 > 0.96$ for all MDC and MIC values. See comparison plot in **Figure S12**.

SNAPP $S16_M$ had consistently lower MDC, MIC and MBC than $S8_M$ indicating that it is more effective. $S16_M$ and $S8_M$ were orders of magnitude lower than those of some of the most common antibiotics

of clinical use (*e.g.* MICs of 11.4 μM for ampicillin and 8.3 μM for kanamycin *versus* this same strain of *E. coli*).[32] In comparison, $S4_M$ showed a much weaker activity than $S16_M$ and $S8_M$, requiring significantly higher concentrations to trigger the same antimicrobial effects. Taking MIC values as comparison, these followed the trend 127 ($S16_M$) < 322 ($S8_M$) < 2,636 ($S4_M$) nM. The SNAPP containing the most arms, $S16_M$, displayed the strongest antimicrobial effect, being 2.5 and 20 times more active than $S8_M$ and $S4_M$, respectively, and likewise $S8_M$ was 8 times more active than $S4_M$. Therefore, it was clear that SNAPPs bearing more polypeptide arms led to stronger antimicrobial activities, as consistently found in all three antimicrobial tests. Based on the cooperative mechanism of action many antimicrobial peptides follow, which self-assemble as oligomers on bacterial membranes to trigger their action,[33] more substituted SNAPPs (*i.e.* with more polypeptide arms) could facilitate the cooperative action of neighbouring polypeptide arms and thus exert their antimicrobial action at lower concentrations. As a comparison, $S16_M$ displayed very similar MBC values as the S16 previously reported by our group: 152 and 170 nM, respectively.[10] This batch comparison confirmed that the optimised synthetic conditions described in this article produced more defined star-shaped polymers, hence allowing a more precise structural exploration of the SNAPPs, while retaining the excellent antimicrobial activities previously observed.

The effect of the arm length of the SNAPPs (*i.e.* DP of the polypeptides) was then evaluated at a constant value of 4 arms per star polymer, as discussed previously. Shorter ($S4_S$) and longer ($S4_L$ and $S4_{VL}$) versions of the $S4_M$ initially tested were prepared (**Table 1**). It was found that $S4_S$ did not cause any antimicrobial effect even at the highest concentration tested (30,000 nM), being the only inactive SNAPP from the whole collection reported in this study (**Table 2**). Given that most natural

antimicrobial peptides consist of *ca.* 10-50 residues,[8] it was not surprising that the short arms of $S4_S$, with an average DP of 5, were unable to damage bacterial cells. In this sense, the arms of $S4_S$ may be below a minimum length required for their interaction with cellular membranes, which has been established at *ca.* 7-8 amino acids for antimicrobial peptides.[34] $S4_L$ and $S4_{VL}$ displayed stronger antimicrobial activities than their shorter 4-armed analogues, with a *ca.* 5-fold reduction in MIC values compared to $S4_M$. It was clear that longer polypeptide arms led to stronger antimicrobial activities for this collection of SNAPPs, as evidenced by their decreasing MICs with increasing arm length: >30,000 ($S4_s$) > 2,636 ($S4_M$) > 560 ($S4_L$) ~ 403 ($S4_{VL}$) nM. It must be noted that the increments in arm length (*i.e.* DP) of the S4 star polymers have a constant value of 7, as indicated by their DPs of 5, 12, 19 and 26 (**Table 1**). On this basis, we observed a transition from inactive ($S4_S$) to weakly active ($S4_M$), to much stronger antimicrobial effects ($S4_L$), and then to a plateauing in activity ($S4_{VL}$) by sequential increments of 7 in the DP of the SNAPPs. Therefore, although the 4-arm SNAPPs overall displayed stronger antimicrobial activities with longer arms, this effect begins to plateau and their activity could only significantly improve by increasing their DP up to a value of *ca*. 20. Based on the cooperative action of antimicrobial polypeptides described before, the weak improvement in antimicrobial activity can be explained by the longer distance between the outer termini of polypeptide arms at higher DPs, thus leading to the apparent dilution of the polypeptides at the surface of SNAPPs. Such effect should be less pronounced on SNAPPs with more arms, for example S8 and S16, since these would require higher DPs to experience the same separation of neighbouring polypeptide arms as a less substituted analogue like S4 (**Figure 2**). This argument assumes there is little entanglement/folding of the polypeptide arms in solution, as a result of their cationic nature and hence electrostatic repulsion. Nevertheless, the antimicrobial activity of the longest and most

active 4-arm SNAPP, $S4_{VL}$, was weaker than that of medium-arm length $S8_M$ and $S16_M$, which implies a stronger contribution of arm number over DP towards more potent antimicrobial effects.

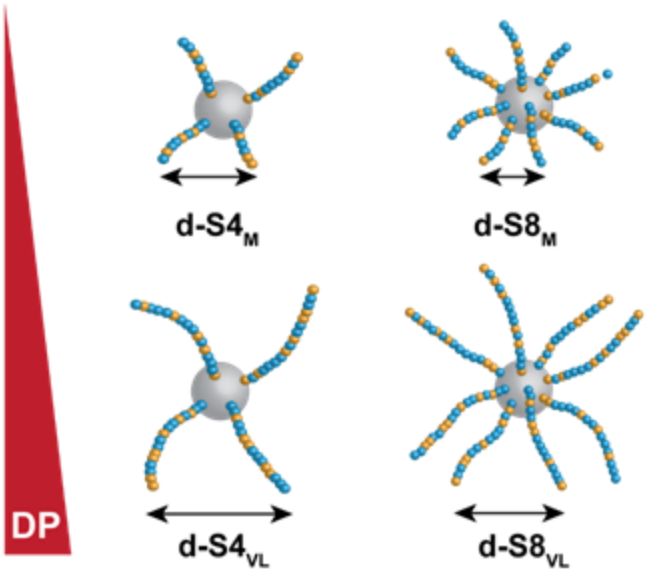


**Figure 2**. Representation of the increase in SNAPP arm distance (d) with DP and its dependence on arm number: d-$S4_{VL}$ > d-$S4_M$ ~ d$S8_{VL}$ > d-$S8_M$.

From the discussion above, it can be anticipated that SNAPPs with both more and longer arms would lead to superior antimicrobial activities. This conclusion encouraged the synthesis of 8- and 16-arm SNAPPs of higher DP to test a potential synergistic effect between these two structural features. Despite successfully preparing an 8-arm very long SNAPP ($S8_{VL}$) (**Table 1,** see also **Figures S6 and S9C** for SEC and DLS data respectively), the synthesis of a 16-arm analogue ($S16_{VL}$) proved to be difficult due to the loss of polymerisation control at high DPs from this more sterically hindered star polymer,

resulting in very high polydispersity (**Figure S7**). A long 16-arm SNAPP ($S16_L$) was investigated instead, which still offered good polymerisation control (**Table 1,** see also **Figures S8 and S9D** for SEC and DLS data respectively). Interestingly, $S8_{VL}$ showed a 17% reduction in MIC compared to our benchmark SNAPP $S16_M$, but more importantly, $S16_L$ displayed the strongest antimicrobial activity from the whole collection tested, with a 45, 33 and 60% reduction in the MDC, MIC and MBC of the parent $S16_M$, respectively (**Table 2**). The outstanding MBC value of 59 nM shown by $S16_L$ demonstrated the synergy between the two structural parameters of SNAPPs under study.

By increasing the arm number, but keeping arm length constant (i.e. $S16_M$, $S8_M$ and $S4_M$) or increasing arm length but keeping arm number constant (i.e. $S4_s$, $S4_M$, $S4_L$ and $S4_{VL}$), would increase the molecular weight of the individual SNAPPs. Molecular weight of chitosan or polymethacrylate polymers has been shown to affect antimicrobial activity but different studies have shown divergent relationships, with studies shown that activity can be positively or negatively correlated to molecular weight.[35, 36] In our study, an increase in arm number or arm length, equating to an increase in SNAPP molecular weight positively correlates with antimicrobial activity. However molecular weight may not be the only factor contributing to activity. For example, increasing the arm length of S8 SNAPP to $S8_{VL}$ resulted in only a 5% increase in molecular weight as compared to $S16_M$, but a 20% increase in antimicrobial activity. In our previous work[10] we found that $S32_M$ had an increase in molecular weight of 180% as compared to $S16_M$ but this resulted in a 80% increase in activity.

In general, the MDC, MIC and MBC values calculated for each SNAPP were very similar, suggesting that their mechanism of action is bactericidal rather than bacteriostatic (*i.e.* growth inhibition),

which is ideal to deliver an effective antimicrobial action *in vivo*. With MDC values being similar to MIC and MBC values, this also indicates that membrane damage is the central mechanism involved in the activity of SNAPPs against bacteria. This action could potentially result in other secondary mechanisms of bacterial cell death such as interference of metabolic functions and synthesis of biomolecules in the cytoplasm, as suggested for analogous antimicrobial peptides,[7] which has been observed previously with SNAPPs.[10]

## 2.3 Mechanisms of action of SNAPPs

To further understand the effects of architecture on the mechanisms of action of each of the SNAPP variants (**Table 1**) we initially characterised the changes in membrane potential in *E. coli* upon incubation with each SNAPP using microbial flow cytometry (**Figure 3A**). In this assay the fluorescent dye $DiOC_2(3)$ intercalates and self-associates in the membrane and exhibits a mixed red/green fluorescence in bacteria maintaining stable membrane potential (**Figure 3A**). In comparison to normal viable bacteria a loss in red fluorescence indicates a depolarised membrane and an increase in red fluorescence is indicative of a hyperpolarised membrane. **Figure 3A** shows the microbial flow cytometry dot plots of *E. coli* cells in a stable, fully depolarised and hyperpolarised membrane potential state. All of the SNAPPs were capable of inducing a depolarised membrane in *E. coli* (**Figure 3B**). Intriguingly, increasing the SNAPP arm length for S16, S8 or S4 resulted in an increase in membrane depolarisation, with $S16_L$ and $S8_{VL}$ inducing depolarisation at the lowest concentrations. As with antimicrobial activity, the effect of arm length would appear to be limited as the depolarisation profile for $S4_L$ and $S4_{VL}$ were similar. Increasing arm number of the SNAPPs also

resulted in an increasing in depolarisation with $S16_M$ > $S8_M$ >> $S4_M$ (**Figure 3B**). For each of the SNAPPs, full depolarisation of the *E. coli* population coincided with the MDC/MIC/MBC values. Although all SNAPPs were able to induce depolarisation, only SNAPPs that had a medium arm length induced hyperpolarisation with $S16_M$ > $S8_M$ >> $S4_M$ (**Figure 3C**). The concentration at which the maximum hyperpolarised membrane state was induced by $S16_M$, $S8_M$ and $S4_M$ was found to be at 50% of the MDC/MIC/MBC values for each of the SNAPPs. This data indicates that although increasing SNAPP arm number increases the ability of the SNAPP to depolarise *E. coli*, mirroring antimicrobial activity (**Table 2**), it is the arm length that has a dual action on membrane potential as only SNAPPs with medium length arms were able to induce a hyperpolarised state prior to inducing a depolarised state. This may indicate that the long arm SNAPPs have a more rapid rate of action than the medium length arm SNAPPs. Further it indicates that the medium length arm SNAPPs induces a state of unregulated ion efflux/influx resulting in a more negatively charged membrane.

Recently it has been shown that hyperpolarisation in mitochondria and yeast cells results in the generation of reactive oxygen species (ROS) leading to cell death.[37] To investigate this *E. coli* cells treated with each of the SNAPP variants were incubated with CellROX orange, which fluoresce upon oxidation by ROS. **Figure 3D** shows a representative microbial flow cytometry dot plot control and oxidatively stressed (CellROX orange positive) *E. coli* cells. In this assay, both $S16_M$ and $S8_M$ induced ROS production in *E. coli* cells (**Figure 3E**). It was also found that $S16_L$ was also capable of inducing ROS production with a similar magnitude of ROS+ bacterial cell population but at a lower concentration than $S8_M$. Unlike the medium length arm SNAPPs, $S16_L$ was found in our assays to not induce hyperpolarisation, indicating that it may act via a different mechanism to the medium length arm SNAPPs. Kohanski *et al* [38] have shown that bactericidal antibiotics that act on internal targets

induce ROS and upregulate the gene *recA,* We have previously shown that S16 does internalise into the cytoplasm of *E. coli* and upregulates *recA.*[10] Our data indicates that $S16_L$ has a rapid mode of action which may result in its internalisation and ROS production via disruption of internal mechanisms in a fashion similar to bactericidal antibiotics. The SNAPP $S16_M$ was found to produce the strongest ROS production in *E. coli* cells.

Taken together our data clearly shows that the antimicrobial mode of action of SNAPPs is primarily one of membrane disruption causing hyperpolarisation and depolarisation of the membrane and subsequent oxidative stress/ROS production and this is influenced by SNAPP arm length and arm number.

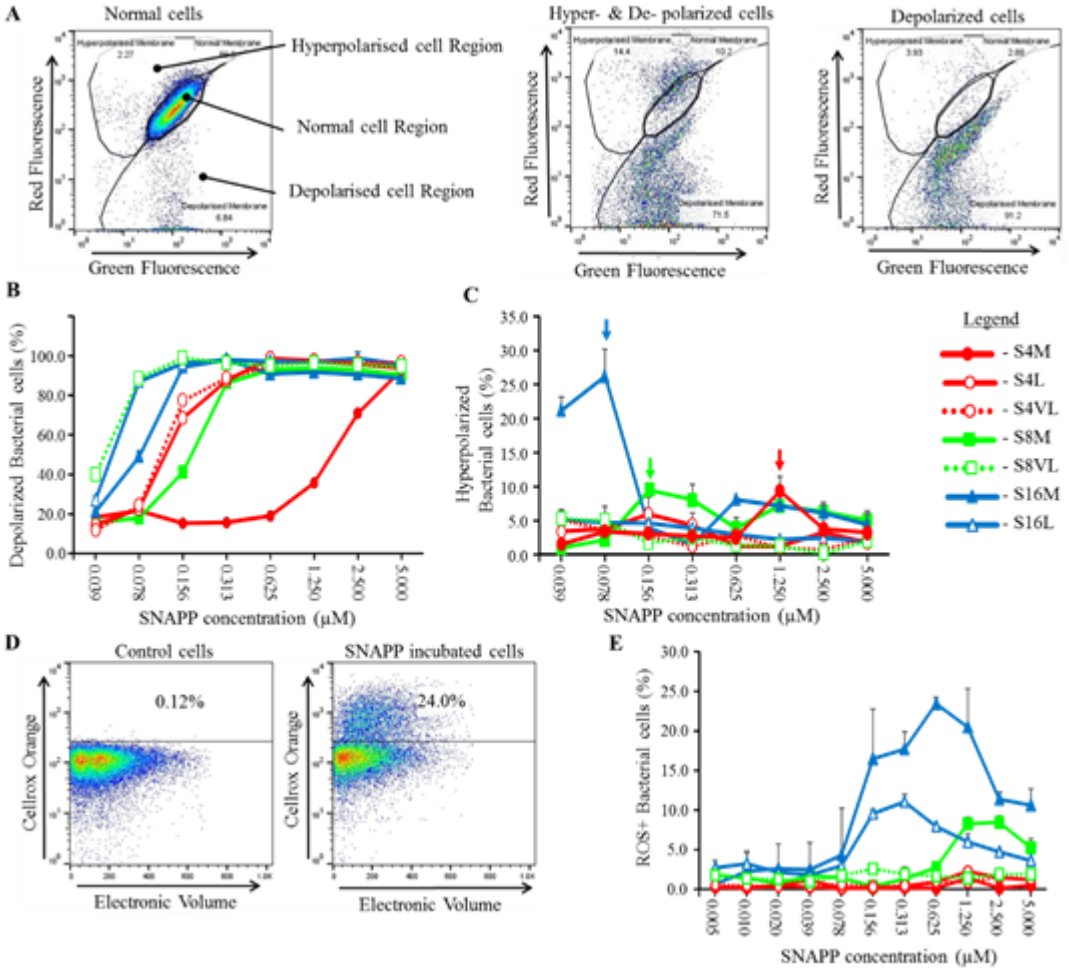


**Figure 3.** SNAPP effect on *E. coli* membrane potential and induction of reactive oxygen species (ROS). A) Representative microbial flow cytometry dot plots showing *E. coli* cells with normal, hyperpolarised and depolarised membrane potential. B) Percent of depolarised *E. coli* cells induced by SNAPP variants. C) Percent of hyperpolarised *E. coli* cells induced by SNAPP variants; arrows indicate maximal point of hyperpolarisation. D) Representative microbial flow cytometry dot plots showing *E. coli* cells with no oxidative stress (control cells) and under oxidative stress (SNAPP incubated cells). E) Percent of reactive oxygen species positive (ROS) *E. coli* cells induced by SNAPP variants. Data is expressed as the mean ± standard deviation; $n = 6$.

2.4 Secondary structure of the polypeptide arms of SNAPPs

Given the critical importance of the secondary structure of many antimicrobial peptides for their activity, which in many cases require an α-helical or β-sheet conformation to create amphiphilic domains for membrane interaction,[33, 34, 39] the secondary structure of the polypeptide arms of SNAPPs was investigated by circular dichroism (CD). The CD spectra of the SNAPPs in aqueous solution did not present the characteristic bands of any particular secondary structure, and all polypeptide arms displayed a random/extended conformation under these conditions (**Figure 4A**).[40] However, upon addition of the co-solvent 2,2,2-trifluoroethanol (TFE), all SNAPPs transitioned into an α-helical conformation. TFE is commonly used for the characterisation of secondary structures by CD, as it displaces water from the surface of peptides and thus promotes intramolecular hydrogen bonding.[41] As such, the CD spectra of peptides in TFE/water mixtures provides an indication of their conformation in more hydrophobic environments, such as those of cellular membranes (*i.e.* lipid bilayers).[42] On this basis, our results suggest that whereas the polypeptide arms of SNAPPs do not present organised secondary structures in aqueous media, they may acquire an α-helical conformation upon binding to bacterial membranes.

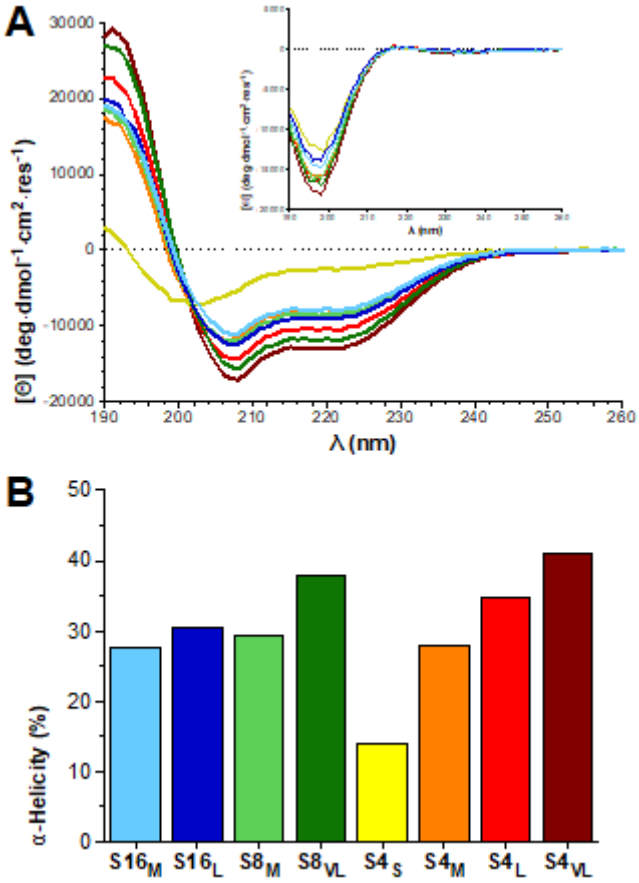


**Figure 4**. A) Circular dichroism spectra of SNAPPs in 80% v/v TFE in water – the inset shows the spectra of the samples in pure water. B) Relative α-helicity of SNAPPs in 80% v/v TFE in water.

The α-helical content of SNAPPs in TFE/water mixtures was estimated from their CD minimum at 222 nm, and it represents the relative number of amino acids in these polypeptides arranged in α-helices (**Figure 4B**). It was found that the α-helical composition of SNAPPs does not depend on the number of polypeptide arms, as evidenced by the constant 28-29% helicity across $S16_M$, $S8_M$ and $S4_M$.

However, the DP of SNAPPs had a strong impact on their secondary structure, and at a constant number of arms, longer polypeptide chains presented higher α-helicities: $S4_S$ (14%) < $S4_M$ (28%) < $S4_L$ (35%) < $S4_{VL}$ (41%); and $S8_M$ (29%) < $S8_{VL}$ (38%). It can be argued that the segment of the polypeptides connected to the core of the SNAPPs should be less flexible than their outer terminus due to steric hindrance, and as such, SNAPPs of higher DP present longer flexible polypeptide segments and hence higher α-helicities. $S16_L$ only showed a subtle increase in helical content compared to $S16_M$ which can be attributed to their small difference in DP (**Table 1**), but it was nevertheless sufficient to endow $S16_L$ with stronger antimicrobial activity.

Our results show that at constant arm number, longer polypeptide arms lead to higher α-helical content for SNAPPs in membrane-mimicking environments, which overall translates into stronger antimicrobial activities. This observation suggests that the higher antimicrobial activities of SNAPPs with increasing DP can be attributed to their increasing helical content. However, the inverse correlation between the α-helical content and MIC values found in the S4 collection was lost at high DP (**Figure 5**): Despite the higher helicity of $S4_{VL}$ as compared to $S4_L$, both SNAPPs showed almost identical MICs. This result could be an effect of the higher separation between polypeptide arms at the surface of SNAPPs with higher DP values, as discussed above (**Figure 2**), which should weaken their antimicrobial activity. Therefore, increasing the DP of SNAPPs leads to stronger antimicrobial effects, probably due to the higher helicity of longer polypeptide arms, but only up to a certain DP beyond which higher helicities are outweighed by the higher separation between polypeptide arms.

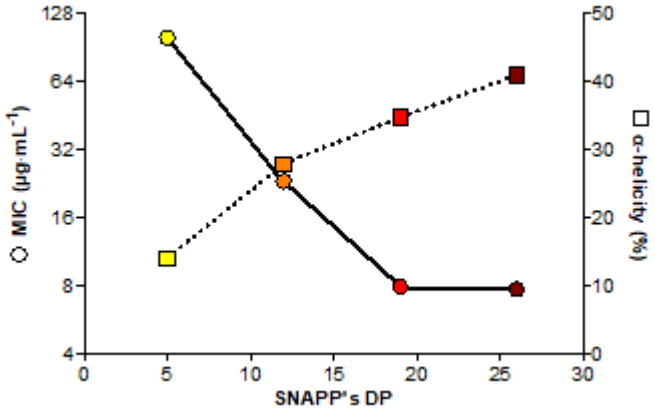


**Figure 5**. MIC *versus* relative α-helicity (%) of 4-arm SNAPPs of different DP: 5 ($S4_S$), 12 ($S4_M$), 19 ($S4_L$) and 26 ($S4_{VL}$).

## 2.5 *In vitro* toxicity of SNAPPs towards mammalian cells

To assess the impact of SNAPP architecture on their biocompatibility, their toxicity towards mammalian cells was evaluated. Rat hepatoma (H4IIE) cells were exposed to SNAPPs and the level of cell apoptosis and cell death was determined by flow cytometry. In this experiment, the green fluorescent dye Yo-Pro®-1 was used to stain cells during the early stages of apoptosis, when their cytoplasmic membrane becomes slightly permeable, whereas the red fluorescent dye PI was used to stain dead cells with damaged membranes. Overall, the cytotoxicity of the SNAPPs increased by having more and longer polypeptide arms, in a similar trend as observed for their antimicrobial activity (**Table 3**). However, the increase in toxicity with more polypeptide arms plateaus at 8 arms across the medium DP collection, as evidenced by the $IC_{50}$ values of $S4_M$ (129.6) > $S8_M$ (46.0) ~ $S16_M$

(44.8), with this effect translating into the SNAPP with the highest therapeutic index in this study being $S16_M$. The increased toxicity of $S16_L$ and $S8_{VL}$ compared to $S16_M$ outweighed the higher antimicrobial activity of the former, and thereby led to lower therapeutic indices for $S16_L$ and $S8_{VL}$. For the S4 SNAPPs, which are the easiest to synthesise as discussed earlier, toxicity does not appear to increase proportionally to antimicrobial activity, leading to an $S4_L$ SNAPP with a similar therapeutic index to the benchmark $S16_M$ (**Table 3**, bold values). The ability to generate easier-to-prepare S4 architectures with similar biological properties to $S16_M$, which showed the highest therapeutic index, offers significant benefits from a manufacturing standpoint.

**Table 3**. Toxicity of SNAPPs against rat hepatoma cells (H4IIE), measured as the concentration that caused the death of 50% of the cell population ($IC_{50}$).

| **SNAPP code** | **MIC (nM)** | **$IC_{50}$ (nM)** | **TI**[a)] |
|---|---|---|---|
| $S16_M$ | 127 | 1,090 | **8.6** |
| $S16_L$ | 85 | 614 | 7.2 |
| $S8_M$ | 322 | 1,966 | 6.1 |
| $S8_{VL}$ | 105 | 702 | 6.6 |
| $S4_S$ | >30,000 | >60,000 | n/a[b)] |
| $S4_M$ | 2,636 | 14,727 | 5.6 |
| $S4_L$ | 560 | 4,454 | **8.0** |
| $S4_{VL}$ | 403 | 2,531 | 6.3 |

[a] The therapeutic index (TI) of each SNAPP was calculated as the ratio between the $IC_{50}$ divided by its MIC against *E. coli* (**Table 2**). [b] TI of $S4_S$ is not available as no MIC could be calculated for this SNAPP.



2.6 *In vivo* toxicity of SNAPPs

To further understand the biocompatibility of SNAPPs, the material with the highest therapeutic index in the collection ($S16_M$) was tested in a murine model. The toxicity of $S16_M$ was assessed *in vivo* by determining the levels of two specific organ damage markers –alanine transaminase (liver) and creatine kinase (kidney)–, and non-specific cell damage markers for allergic reactions (histamine) and necrosis (adenosine triphosphate or ATP), measured in the blood and peritoneal fluid of mice. No detectable levels of alanine transaminase, creatinine kinase or histamine were detected in the blood nor peritoneal fluid of mice after treatment with $S16_M$. However, significant levels above control (PBS injection) of ATP were detected in the peritoneal fluid of mice treated with 4 $mg \cdot kg^{-1}$ of $S16_M$ (**Figure 6**).

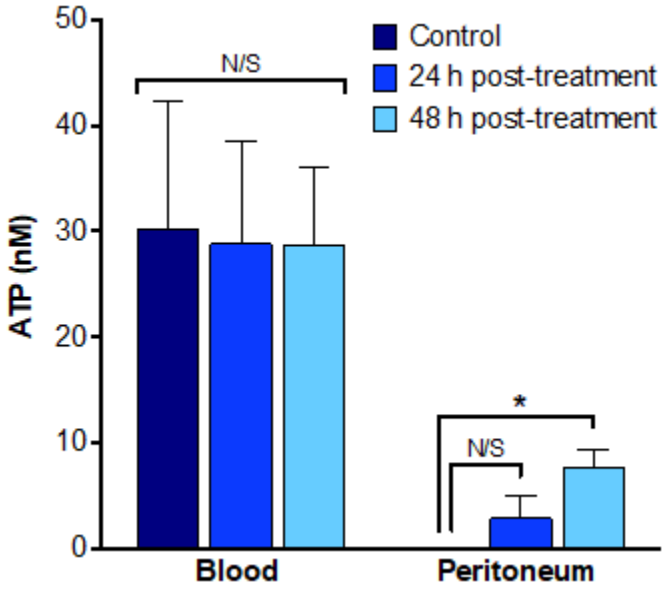


**Figure 6**. Concentrations of ATP found in the blood and peritoneum of mice receiving no treatment (PBS, control) and after administration of $S16_M$ (24 and 48 h post-treatment). Each bar represents the mean ± standard deviation, *n* = 10. Statistical significance was determined not significant ('N/S') and * $p < 0.1$.

The *in vivo* toxicity results suggest that $S16_M$ was able to cause localised tissue damage resulting in the release of ATP into the peritoneal cavity, as evidenced by the sustained increase in the levels of this marker after 24 and 48 hours. However, the lack of detectable increase in alanine transaminase and creatinine kinase, or even ATP in blood, suggests the SNAPP had a localised effect at the site of injection. Elevated levels of ATP, as observed in the peritoneal cavity in this study, may have several immunological effects: High levels of extracellular ATP act as a damage-associated molecular

pattern, able to be detected by certain cells of the immune system that express the appropriate P2 receptor.[43, 44] In the peritoneal cavity, the main resident immune cells are macrophages.[45] Ligation of ATP by P2 receptors on macrophages results in their activation and recruitment of immature monocytes from the bloodstream.[43] During an inflammatory response in the peritoneum, the first cells recruited are circulating blood neutrophils, and it has been demonstrated that extracellular ATP modulates neutrophil vascular adhesion and extravasation into surrounding tissue.[46, 47] Therefore, it is likely that the production of extracellular ATP upon administration of SNAPP to the peritoneal cavity contributes to the influx of neutrophils previously observed *in vivo.*[10] This *in vivo* data demonstrates the very high biocompatibility of SNAPPs and suggests that they have a multi-modal action through both direct killing (via interaction with the bacterial membrane) and indirect killing by inducing a localised increase in ATP levels which drive immune cells to the site of infection and facilitate bacterial clearance.

**3. Conclusions**

A library of star-shaped SNAPPs with systematic modifications in arm number and DP was successfully synthesised to study their architectural effects on biological activity. Overall, it was found that SNAPPs bearing more and longer polypeptide arms displayed stronger antimicrobial effects characterised by high levels of membrane depolarisation. The stronger activity of SNAPPs with more and longer arms was attributed to their higher densities of polypeptide chains and α-helical contents, respectively. However, the improvement in antimicrobial activity with DP saturates,

probably as a result of the higher separation between longer polypeptide arms. These observations led to the design of two more potent SNAPPs, $S16_L$ and $S8_{VL}$, displaying up to 60% increase in antimicrobial activity compared to our early benchmark polymer, $S16_M$. However, arm length had an effect on the mode of action with long and very long armed SNAPPs resulting in membrane depolarisation whereas, medium arm length SNAPPs induced a hyperpolarised state in *E. coli* prior to full depolarisation. This data suggests that by modifying the SNAPP arm architecture there is potential to tune the mechanism of action of the SNAPPs. The *in vitro* toxicity of SNAPPs also increased with more and longer polypeptide arms, however, we were able to identify an easier-to-prepare 4-arm SNAPP with similar therapeutic index to the highest found across the collection. The *in vivo* evaluation of the SNAPP with the highest therapeutic index showed no indication of systemic organ damage, while causing a local release of ATP that may contribute to activate the immune system and tackle infection. In summary, this paper constitutes the first in-depth study into the structure-activity relationships of this promising class of antimicrobial polymers and sets the basis for the future development of SNAPPs with improved biological properties.

**5. Experimental Section**

*Materials:* H-L-Lys(Z)-OH (Mimotopes), D,L-Valine (>99%, Acros Organics), diethyl ether (Chem-Supply), generation 0 poly(amido amine) dendrimer (G0 PAMAM) (Dendritech), generation 1 poly(amido amine) dendrimer (G1 PAMAM) (Dendritech), generation 2 poly(amido amine) dendrimer (G2 PAMAM) (Sigma), *bis*(trichloromethyl)carbonate (triphosgene, 99%, Aldrich), trifluoroacetic acid (TFA) (99%, Aldrich), hydrobromic acid (33% in acetic acid) (Aldrich), *n*-pentane (anhyd., >99%, Aldrich), *n*-butyl alcohol (Chem-Supply), sodium bicarbonate (Chem-Supply), Phenol red-free Dulbecco's Modified Eagle Medium (DMEM) (Sigma), Dulbecco's Phosphate-Buffered Saline (DPBS) (Sigma), trypsin-ethylenediaminetetraacetic acid (EDTA) (Sigma), Fetal Bovine Serum (Sigma) and Mueller-Hinton Broth (MHB) (Oxoid). Dimethyl sulfoxide (DMSO) (anhyd., Aldrich) and *N*,*N*-dimethylformamide (DMF) (anhyd., Acros Organics) were stored under activated 4A molecular sieves. Tetrahydrofuran (THF) (Chem-Supply) was distilled from benzophenone and sodium metal under nitrogen before use. Ethyl acetate (EtOAc) (Chem-Supply) was distilled from calcium hydride before use. SnakeSkin™ dialysis tubing 3,500 MWCO, Syto®9 and membrane permeability/dead cell apoptosis kit (Yo-Pro®-1 and propidium iodide (PI)) were purchased from Thermo Fisher Scientific. Detection kits for alanine transaminase (ab105134), creatine kinase (ab155901), histamine (ab213975) and ATP (ab83355) were purchased from Abcam.

*Instrumentation:* $^{1}$H NMR analysis was performed using a Varian unity Plus 400 MHz NMR spectrometer using the deuterated solvent as reference. Size exclusion chromatography (SEC) analysis was performed on an aqueous gel permeation chromatography (GPC) units using an eluent of Milli-Q water containing 0.1% v/v trifluoroacetic acid (TFA). The system was operated at a flow rate of 1 mL · min$^{-1}$ at 25 °C. A Shimadzu Liquid Chromatography system was utilized, equipped with a Shimadzu RID-10 refractometer (λ = 633 nm) and Wyatt 3-angle light scattering detector, with three Waters Ultrahydrogel columns in series ((i) 250 Å porosity, 6 µm diameter bead size; (ii) and (iii) linear, 10 µm diameter bead size) for separation. The dn/dc values of the $S4_M$, $S8_M$, and $S16_M$ SNAPPs were calculated to be 0.187, 0.183, 0.188 respectively at 25 °C using a batch injection protocol and Wyatt ASTRA SEC/LS software. Molecular weight and polydispersity values were calculated on the Wyatt ASTRA SEC/LS software package using Debye modelling with a fit of 2. All GPC samples prepared at a concentration of 5 mg · mL$^{-1}$ and were filtered through 0.45 µm nylon filters prior to injection. DLS and zeta potential measurements were performed on a Malvern Zetasizer Nano ZS with 4.0 mW HeNe laser operating at 632.8 nm. Analysis was performed at an angle of 173° at a constant temperature of 25 ± 0.01 °C. Samples were made at a concentration of 0.5-2 mg · mL$^{-1}$ in DMEM (the same media conducted for antibacterial studies) depending on the sample so that reliable correlation functions were obtained. Zeta potential measurements were performed at

concentrations of 2 mg · $mL^{-1}$ in DI water. Measurements were performed in triplicate. All samples filtered through 0.45 µm nylon filters prior to measurement. MIC values were calculated using a Multiskan Ascent (Labsystems) microplate reader. MDC values were calculated by flow cytometry using a Quanta SC MPL (Beckman Coulter Pty, Ltd) equipped with a 100-W stabilised mercury arc lamp with wavelengths of 365, 404, and 435 nm, and a 488-nm diode laser. CD spectra were recorded on a Chirascan™-plus (Applied Photophysics Ltd) at 25°C between 190-260 nm, scanned in 1 nm steps and measuring the absorbance during 0.5 sec per step. The *in vitro* cytotoxicity of SNAPPs was measured by flow cytometry on a LSRFortessa X-20 (Becton Dickinson). Colourimetric assays for metabolite quantification (i.e. *in vivo* biocompatibility experiment) were performed on a Wallac 1420 Multilabel Counter microplate reader (Perkin Elmer).

*Synthesis of D,L-Valine and (Z)-L-Lysine N-Carboxyanhydrides (NCAs):* ε-(Z)-L-Lysine and D,L-Valine NCAs were synthesized as per our previously reported procedure,[24] with the inclusion of an additional purification step reported by Poche *et al*. to remove hydrochloride impurities from the reaction.[48] Dried H-L-Lys(Z)-OH (2 g, 7.14 mmol) or D,L-Valine (2 g, 17.0 mmol)) were suspended in anhydrous THF (50 mL) in a three-necked round bottomed flask under argon. Triphosgene (lys: 0.85 g, 2.86 mmol, 1.2 equiv. phosgene; val: 2.0 g, 6.74 mmol, 1.2 equiv. phosgene) was then added and the mixture was refluxed at 65 °C for 2 h with continuous stirring. After cooling to room temperature, the reaction mixture was sparged with argon for 45 mins into a sat. NaOH solution, then solvent removed completely *in vacuo* to a white solid. The solid was then suspected in EtOAc (50 mL, anhydrous), chilled and placed into a separator funnel where the crude NCA solution was gently washed with chilled saturated brine solution (50 mL), and 0.5 % w/v $NaHCO_3$ solution (50 mL). The organic phase was then dried with $MgSO_4$, filtered and concentrated to an oil under low heat, and re-crystalized (x2) from EtOAc (anhydrous) and *n*-pentane (anhydrous). The resulting crystals were then filtered and washed with *n*-pentane (dry). The crystals were then re-dissolved in minimal EtOAc, filtered, precipitated and washed with dry *n*-pentane to afford white powder solids (Yields: ~80 %) $^1$H NMR (400 MHz, $CDCl_3$): (Z)-L-Lysine NCA: $\delta_H$ 1.40-1.60 (m, 4H, NH-$CH_2$-$CH_2$-C$H_2$-C$H_2$-), 1.81-1.94 (m, 2H, NH-$CH_2$-C$H_2$-$CH_2$-$CH_2$-), 3.18 (m, 2H, NH-C$H_2$-$CH_2$-$CH_2$-$CH_2$-), 4.25 (t, 1H, *J* = 4.0 Hz, C*H*N), 4.97 (s, 1H, side chain NH), 5.09 (s, 2H, C$H_2$-ArH), 7.04 (s, 1H, ring NH), 7.3-7.4 (m, 5H, ArH). m.p. 80-82 °C (Lit. m.p. 80 °C).[49] D,L-Valine NCA : $\delta_H$ 1.02 (d, 3H, *J*= 8.0 Hz, C$H_3$), 1.08 (d, 3H, *J*= 8.0 Hz, C$H_3$), 2.25 (m, 1H, C*H*($CH_3$)$_2$), 4.22 (d, 1H, *J* = 4.0 Hz, C*H*-NH), 6.95 (s, 1H, CO-N*H*). m.p. 99-100 °C (Lit. m.p 99 °C).[50]

*General procedure for synthesis of (PZLL–r-PVal)$_{arm}$ PAMAM–(NH$_2$)$_{m,core}$:* In line with previously our previously reported work,[10] a theoretical lysine-to-valine ratio of approximately 2.5:1 was targeted. To account for different observed reactivity rates of the two monomers, Lys NCA and Val NCA in approximately 2:1 molar ratio were both dissolved in anhydrous DMF ([NCA]$_{total}$ = ~55 mg/mL) and added via syringe to a test tube containing PAMAM-(NH$_2$)$_m$ (dried) dissolved completely in anhydrous DMSO (volume corresponding to 10% v/v of final reaction volume) under $N_2$. The test tube was then immersed in an ice chest and stirred for 24 h in ice under constant nitrogen flow and with a bleed for $CO_2$ removal (Note: S8$_{VL}$ was stirred for total 50 h). *n*-butyl alcohol (0.86 µL/mg of NCA$_{total}$ added to reaction) was then added to quench remaining NCA monomer and the mixture stirred for a further 1 h. The reaction mixture was then concentrated under vacuum and transferred into diethyl ether to precipitate. The precipitate was then washed thoroughly with ether and dried *in vacuo* to afford an off-white solid. Average yield ~60%.

*General deprotection to prepare (PLL–r-PVal)$_{arm}$ PAMAM–(NH$_2$)$_{m,core}$:* Protected star polymer was first fully dissolved in TFA (5 mL/g polymer). 33% HBr in acetic acid was then added (10 mL/g polymer), the reaction mixture stoppered and stirred at room temperature with precipitate forming soon after. After stirring for a total of 2 h at room temperature, the solution was added directly into diethyl ether, washed further in ether (x2) and dried under vacuum. The dried solid was then dissolved up in minimal DI water, transferred to 3.5 kDa dialysis tubing and dialysed against a large volume of DI water (~180 times volume of original dialysis content)(x3) for 24 h. The dialysed solutions were then lyophilised to obtain the deprotected SNAPP as a dried white solid. $^1$H NMR (400 MHz, $D_2O$): $\delta_H$ 0.9 (s, 2(C*H*)$_3$), 1.3-1.9 (m, NH-CH$_2$-C*H$_2$*-C*H$_2$*-C*H$_2$*-), 2.0 (br s, C*H*-NH valine), 3.0 (s, NH-C*H$_2$*-CH$_2$-CH$_2$-CH$_2$-), 4.0-4.15 (s, C*H*-NH backbone valine), 4.2-4.4 (s, C*H*-NH backbone lysine). See Figure S3 for example $^1$H NMR spectra of deprotected star SNAPP (S16$_M$).

*Antimicrobial assays – General sample preparation:* 150 µL of serial 2-fold dilutions of SNAPPs (200-3.12 mg · $mL^{-1}$) in DMEM were added to a 96-well microplate. An inoculum of *Escherichia coli* (ATCC® 25922) in MHB was incubated at 37°C with orbital shaking (200 rpm) for 2 h to reach exponential growth. After this time, the culture was diluted with DMEM to give final concentration of $2.5 \cdot 10^6$ cells · $mL^{-1}$, and 150 µL of this stock of bacteria were mixed with the SNAPP dilutions in the microplate, to give a final mixture of bacteria and SNAPP (100-1.56 mg · $mL^{-1}$) of 300 µL. A sample of bacteria without SNAPP was prepared likewise as negative antimicrobial control by replacing the SNAPP solution with neat DMEM. This microplate was incubated at 37°C standing still for 90 min. After this time, the MIC, MDC and MBC experiments described below were performed. The results from all antimicrobial assays described herein were collected from two independent experiments (*i.e*. biological replicates), each of which contained five (MIC and MDC) or three (MBC) technical replicates.

*Minimum Inhibitory Concentration (MIC):* After 90 min of incubation (see "Antimicrobial assays – General sample preparation" above), 100 µL of the SNAPP and bacteria mixtures were diluted with the same volume of MHB in a new microplate. This microplate was incubated at 37°C with orbital shaking (180 rpm) in a microplate reader, and the optical density at 630 nm ($OD_{630}$) of the samples was read every 20 min over 20 h. The $OD_{630}$ of the samples at the time point were the control without SNAPP finished exponential growth were normalised to the $OD_{630}$ of this control (100% relative growth), plotted against SNAPP concentration and fitted to an exponential regression (Figure S13). The MIC was defined as the lowest concentration of SNAPP that inhibited 99% of bacterial growth, and was determined as the concentration that corresponded to 1% relative growth in the exponential regression of the data.

*Minimum Disruptive Concentration (MDC):* After 90 min of incubation (see "Antimicrobial assays – General sample preparation" above), 100 µL of the SNAPP and bacteria mixtures were diluted with 100 µL of DPBS containing 0.1% v/v of Syto®9 (3.34 mM stock solution) and propidium iodide (50 µg · $mL^{-1}$ stock solution). These samples were incubated for 10 min in the dark at room temperature, to be then analysed by flow cytometry measuring Syto®9 emission at 525 nm (fluorescence channel 1, FL-1) and propidium iodide emission at 670 nm (fluorescence channel 3, FL-3). A sample of bacteria treated for 30 min with 70% v/v ethanol in water, centrifuged and resuspended in DMEM, was analysed likewise as positive control for membrane damage. The MDC was defined as the lowest concentration of SNAPP that caused membrane damage in 99% of the bacterial cells and was determined as the concentration that corresponded to a normalised 99% propidium iodide-positive (PI+) cells (Figure S14).

*Minimum Bactericidal Concentration (MBC):* After 90 min of incubation (see "Antimicrobial assays – General sample preparation" above), the SNAPP and bacteria mixtures were serially diluted 10-fold four times in DPBS. 10 µL of each dilution were spotted on MHB agar plates and incubated at room temperature and/or 37°C until individual colonies were visible. Bacterial colonies, or colony forming units (CFUs), were counted at the dilution that allowed to count the most individual colonies without significant overlap between them. The MBC was defined as the lowest concentration of SNAPP that caused a decrease of 99% in viable bacterial cells (i.e. $CFU \cdot mL^{-1}$) as compared to a control sample in the absence of SNAPP (Figure S15).

*Membrane potential assay.*

Membrane potential was determined by microbial flow cytometry using a BacLight Bacterial Membrane Potential Kit (Invitrogen) as previously described.[10] Bacteria that are maintaining a membrane potential (healthy/viable bacteria) the dye $DiOC_2(3)$ intercalates and self-associates in the membrane and exhibits a mixed red/green fluorescence. With a depolarised membrane the $DiOC_2(3)$ dye loses red fluorescence's, whereas in hyperpolarised membranes the $DiOC_2(3)$ increases red fluorescence as compared to normal cells. *E. coli* was harvest at late exponential phase and viable cells were diluted to $2.5 \times 10^6$ cells/mL in PBS and added with serial dilutions of each of the SNAPPs (**Table 1**). A fully depolarized control was provided by the addition of the proton ionophore carbonyl cyanide 3-chlorophenylhydrazone (CCCP) at a final concentration of 5 mM to the untreated cells. Prior to a 1 h incubation at 37 °C, 30 mM $DiOC_2(3)$ was added to all of the samples. Membrane potential was determined by a Cell Lab Quanta SC MPL flow cytometer (Beckman Coulter) as a ratio

of cells that exhibited a red fluorescence (FL-3) to those that displayed a green fluorescence (FL-1). Gates were drawn based on the untreated (polarized) and CCCP-treated (fully depolarized) controls. Data is representative of three independent assays completed in duplicate.

*Determination of reactive oxygen species (ROS) production in bacteria.*

*E. coli* cells were harvest at late exponential phase and viable cells were diluted to $2.5 \times 10^6$ cells/mL in MEM and 100 µL of the bacteria solution was added to each well containing either MEM (untreated control) or serial dilutions of each of the SNAPPs (**Table 1**) (100 µL) and incubated at 37 °C for 90 min. The cells were then stained with the CellROX® Orange Reagent at a final concentration of 750 nM following manufacturer's instructions and were incubated for 1 h at 37 °C. The cells were analysed on the Cell Lab Quanta SC MPL flow cytometer (Beckman Coulter) where the fluorescence from the CellROX® Orange Reagent was measured on FL-3. A minimum of three independent experiments of the assay were conducted and two technical replicates were used in each experiment. Data is expressed as mean ± standard deviation.

*Circular dichroism spectra of SNAPPs:* The secondary structure of SNAPPs was measured from 0.2 $mg \cdot mL^{-1}$ samples in triplicate from a 1 mm-path length quartz cuvette at 25°C. The absorbance of the solvent (*i.e.* blank) was subtracted from the measured ellipticity of the samples (in mdeg), then the spectra were normalised to a value of '0' ellipticity at 260 nm, and the resulting blank-corrected and normalised ellipticity (θ) was converted into mean residual ellipticity ([θ]) using Equation 1[40]:

$$[\theta] = \frac{\theta}{DP \cdot NA \cdot c \cdot \text{path length}} \qquad (Eq. 1)$$

In *Eq*. 1, '*DP*' represents to the average degree of polymerisation of the polypeptide arms of the SNAPP (**Table 1**), '*NA*' indicates the number of arms per SNAPP, '*c*' is the concentration of the SNAPPs in $moles \cdot L^{-1}$, and the '*path length*' of the cuvette in millimetres. Thus, mean residual ellipticities ([θ]) are expressed in the units $deg \cdot cm^2 \cdot res^{-1} \cdot dmol^{-1}$.

The relative α-helicity of the polypeptides was calculated from the mean residual ellipticity of the SNAPPs at 222 nm ($[\theta]_{222}$) measured in 80% v/v TFE in water using Equation 2[51]:

$$\alpha - \text{helicity}\ (\%) = \frac{[\theta]_{222} - 3{,}000}{-39{,}000} \cdot 100 \qquad (Eq. 2)$$

*In vitro toxicity of SNAPPs towards mammalian cells:* The H4IIE cell was chosen for this study as it is a recognised cell line for toxicity testing by retaining its primary cell phenotype.[52] Further to this, as a murine cell line it complements our in vivo murine testing. H4IIE cells were removed from tissue culture flasks with 0.25% trypsin-EDTA solution and resuspended in DMEM containing 10% Fetal Bovine Serum at $1 \cdot 10^6$ cells $\cdot$ mL$^{-1}$ and allowed to recover for 1 hour at 37°C, 5% v/v $CO_2$. Removal of adherent cells can damage the cell membrane and cause false positive results and a one hour incubation was found to reverse any transient-trypsin induced membrane disruption. Increasing concentrations of SNAPPs were added to the cell suspensions which were then incubated at 37°C, 5% v/v $CO_2$ for 90 min. After this time, Membrane Permeability/Dead Cell Apoptosis Kit (Yo-Pro®-1 and propidium iodide) was used as indicated by the supplier, and fluorescence was measured by flow cytometry. Each sample was analysed as two biological replicates, each containing three technical replicates ($n$ = 6).

*In vivo toxicity of SNAPPs on a murine model:* Mice (C57/BL6, 10-12 week old) were given an intraperitoneal injection of 4 $mg \cdot kg^{-1}$ SNAPP $S16_M$ in a total volume of 200 µL (DMEM) using a 25G needle. Intra-peritoneal injection was chosen for toxicity testing as the abdominal cavity is the injection site for the initiation of abdominal sepsis models and for subsequent treatments during a sepsis model. After 24 and 48 hours, mice were killed by $CO_2$ asphyxiation before being bled by cardiac puncture. Sterile, cold DPBS (3 mL) was then injected into the peritoneal cavity with a 19G needle, allowed to incubate for 5 minutes with gentle agitation before being recovered. Blood samples were allowed to coagulate on ice before the serum was aspirated after centrifugation at 5000 g for 5 minutes at 4°C and stored at -20°C for analysis. Peritoneal fluid was aspirated after centrifugation at 5000 x g for 5 minutes at 4°C and frozen at -20°C for analysis. Levels of alanine transaminase, creatine kinase, histamine and ATP were determined from these samples using specific assay kits (see Materials), used according to the manufacturer's instructions. Ten mice were used per group. All animal experiments were approved by The University of Melbourne Ethics Committee for Animal Experimentation.

*Statistical analysis*: Data normalisation is explained in Eq. 2 (CD data) and Fig. S13-S14 (MIC and MDC data). Results are presented as indicated in the corresponding figure captions (*e.g.* mean value ± SD for a sample size 'n'). Statistical analysis was performed with Prism v6.0h (GraphPad Software Inc), and it corresponds to a two-way ANOVA with Fisher's LSD multiple comparisons test at a 95% confidence interval (Fig. 6).

**Supporting Information**

Size exclusion chromatograms, dynamic light scattering data and correlograms, example $^{1}$H NMR spectra of SNAPP, descriptions of MIC, MBC and MDC calculations is available from the Wiley Online Library or from the author.

**Acknowledgements**

The authors would like to thank the Australian Research Council (ARC) for funding in the form of a Discovery Project (DP160101312). The authors would also like to thank Prof. Frances Separovic for access to a CD spectrophotometer.

‡ These authors contributed equally (S.J.S and I.I)

Received: ((will be filled in by the editorial staff))
Revised: ((will be filled in by the editorial staff))
Published online: ((will be filled in by the editorial staff))

References

[1] E. D. Brown, G. D. Wright, *Nature* **2016**, *529*, 336-343.

[2] World Health Organization, *Antimicrobial Resistance: Global Report on Surveillance*, (WHO,2014)

[3] World Health Organization, *Antibacterial Agents in Clinical Development: An analysis of the antibacterial clinical development pipeline, including tuberculosis*, (WHO,2017)

[4] World Health Organization, *Global Priority List of Antibiotic-Resistant Bacteria to Guide Research, Discover, and Development of New Antibiotics*, (WHO,2017)

[5] L. Czaplewski, R. Bax, M. Clokie, M. Dawson, H. Fairhead, V. A. Fischetti, S. Foster, B. F. Gilmore, R. E. W. Hancock, D. Harper, I. R. Henderson, K. Hilpert, B. V. Jones, A. Kadioglu, D. Knowles, S. Ólafsdóttir, D. Payne, S. Projan, S. Shaunak, J. Silverman, C. M. Thomas, T. J. Trust, P. Warn, J. H. Rex, *Lancet Infect. Dis.*, *16*, 239-251.

[6] K. Kuroda, G. A. Caputo, *Wiley. Interdiscip. Rev. Nanomed. Nanobiotechnol.* **2013**, *5*, 49-66.

[7] C. D. Fjell, J. A. Hiss, R. E. W. Hancock, G. Schneider, *Nat. Rev. Drug. Discov* **2011**, *11*, 37.

[8] R. E. W. Hancock, H.-G. Sahl, *Nat. Biotechnol.* **2006**, *24*, 1551-1557.

[9] Z. Y. Ong, N. Wiradharma, Y. Y. Yang, *Adv. Drug Del. Rev.* **2014**, *78*, 28-45.

[10] S. J. Lam, N. M. O'Brien-Simpson, N. Pantarat, A. Sulistio, E. H. H. Wong, Y.-Y. Chen, J. C. Lenzo, J. A. Holden, A. Blencowe, E. C. Reynolds, G. G. Qiao, *Nat. Microbiol.* **2016**, *1*, 16162.

[11] M. D. Wyrsta, A. L. Cogen, T. J. Deming, *J. Am. Chem. Soc.* **2001**, *123*, 12919-12920.

[12] C. Zhou, X. Qi, P. Li, W. N. Chen, L. Mouad, M. W. Chang, S. S. J. Leong, M. B. Chan-Park, *Biomacromolecules* **2010**, *11*, 60-67.

[13] M. Xiong, M. W. Lee, R. A. Mansbach, Z. Song, Y. Bao, R. M. Peek, Jr., C. Yao, L.-F. Chen, A. L. Ferguson, G. C. L. Wong, J. Cheng, *Proc. Natl. Acad. Sci. U.S.A.* **2015**, *112*, 13155-13160.

[14] P. Li, C. Zhou, S. Rayatpisheh, K. Ye, Y. F. Poon, P. T. Hammond, H. Duan, M. B. Chan-Park, *Adv. Mater.* **2012**, *24*, 4130-4137.

[15] A. C. Engler, A. Shukla, S. Puranam, H. G. Buss, N. Jreige, P. T. Hammond, *Biomacromolecules* **2011**, *12*, 1666-1674.

[16] W. Vayaboury, O. Giani, H. Cottet, A. Deratani, F. Schue, *Macromol. Rapid Commun.* **2004**, *25*, 1221-1224.

[17] J. J. Cheng, T. J. Deming, "Synthesis of Polypeptides by Ring-Opening Polymerization of alpha-Amino Acid N-Carboxyanhydrides", in *Peptide-Based Materials*, T. Deming, Ed., Springer-Verlag Berlin, Berlin, 2012, 1-26.

[18] K. Kuroda, G. A. Caputo, W. F. DeGrado, *Chem. Eur. J.* **2009**, *15*, 1123-1133.

[19] K. Kuroda, W. F. DeGrado, *J. Am. Chem. Soc.* **2005**, *127*, 4128-4129.

[20] Y. Oda, S. Kanaoka, T. Sato, S. Aoshima, K. Kuroda, *Biomacromolecules* **2011**, *12*, 3581-3591.

[21] M. Byrne, P. D. Thornton, S.-A. Cryan, A. Heise, *Polymer Chemistry* **2012**, *3*, 2825-2831.

[22] W. Tansey, S. Ke, X. Y. Cao, M. J. Pasuelo, S. Wallace, C. Li, *J. Controlled Release* **2004**, *94*, 39-51.

[23] S. H. Wibowo, A. Sulistio, E. H. H. Wong, A. Blencowe, G. G. Qiao, *Adv. Funct. Mater.* **2015**, *25*, 3147-3156.

[24] S. J. Shirbin, S. J. Lam, N. J.-A. Chan, M. M. Ozmen, Q. Fu, N. O'Brien-Simpson, E. C. Reynolds, G. G. Qiao, *ACS Macro Lett.* **2016**, *5*, 552-557.

[25] A. Sinaga, T. A. Hatton, K. C. Tam, *Biomacromolecules* **2007**, *8*, 2801-2808.

[26] H. R. Kricheldorf, C. von Lossow, G. Schwarz, *Macromolecules* **2005**, *38*, 5513-5518.

[27] R. Muller, C. Laschober, W. W. Szymanski, G. Allmaier, *Macromolecules* **2007**, *40*, 5599-5605.

[28] P. K. Maiti, T. Cagin, G. F. Wang, W. A. Goddard, *Macromolecules* **2004**, *37*, 6236-6254.

[29] N. M. O'Brien-Simpson, N. Pantarat, T. J. Attard, K. A. Walsh, E. C. Reynolds, *Plos One* **2016**, *11*

[30] I. Wiegand, K. Hilpert, R. E. W. Hancock, *Nat. Protoc* **2008**, *3*, 163.

[31] P. Eyer, M. Eddleston, H. Thiermann, F. Worek, N. A. Buckley, *Br. J. Clin. Pharmacol.* **2008**, *66*, 451-452.

[32] M. European Committee for Antimicrobial Susceptibility Testing of the European Society of Clinical, D. Infectious, *Clin. Microbiol. Infect.* **2003**, *9*, ix-xv.

[33] K. A. Brogden, *Nat. Rev. Microbiol.* **2005**, *3*, 238-250.

[34] A. A. Bahar, D. Ren, *Pharmaceuticals (Basel, Switzerland)* **2013**, *6*, 1543-1575.

[35] S. Y., Y. D.I., J. J., *J. Appl. Polym. Sci.* **2001**, *80*, 2495-2501.

[36] J. Kingkaew, S. Kirdponpattara, N. Sanchavanakit, P. Pavasant, M. Phisalaphong, *Biotechnology and Bioprocess Engineering* **2014**, *19*, 534-544.

[37] D. V. Pyatrikas, I. V. Fedoseeva, N. N. Varakina, T. M. Rusaleva, A. V. Stepanov, A. V. Fedyaeva, G. B. Borovskii, E. G. Rikhvanov, *FEMS Microbiol. Lett.* **2015**, *362*

[38] M. A. Kohanski, D. J. Dwyer, B. Hayete, C. A. Lawrence, J. J. Collins, *Cell* **2007**, *130*, 797-810.

[39] M. Zasloff, *Nature* **2002**, *415*, 389.

[40] N. J. Greenfield, *Nat. Protoc* **2006**, *1*, 2876-2890.

[41] D. Roccatano, G. Colombo, M. Fioroni, A. E. Mark, *Proc. Natl. Acad. Sci. U.S.A.* **2002**, *99*, 12179-12184.

[42] B. Deslouches, S. M. Phadke, V. Lazarevic, M. Cascio, K. Islam, R. C. Montelaro, T. A. Mietzner, *Antimicrob. Agents Chemother.* **2005**, *49*, 316-322.

[43] B. N. Cronstein, L. Daguma, D. Nichols, A. J. Hutchison, M. Williams, *J. Clin. Invest.* **1990**, *85*, 1150-1157.

[44] M. J. L. Bours, E. L. R. Swennen, F. Di Virgilio, B. N. Cronstein, P. C. Dagnelie, *Pharmacol. Ther.* **2006**, *112*, 358-404.

[45] A. d. A. Cassado, M. R. D'Império Lima, K. R. Bortoluci, *Front. Immunol* **2015**, *6*, 225.

[46] D. R. Freyer, L. A. Boxer, R. A. Axtell, R. F. Todd, *J. Immunol.* **1988**, *141*, 580-586.

[47] N. C. Kaneider, B. Mosheimer, N. Reinisch, J. R. Patsch, C. J. Wiedermann, *Throm. Res*, *114*, 185-194.

[48] D. S. Poche, M. J. Moore, J. L. Bowles, *Synth. Commun.* **1999**, *29*, 843-854.

[49] W. H. Daly, D. Poche, *Tetrahedron Lett.* **1988**, *29*, 5859-5862.

[50] D. Huesmann, A. Birke, K. Klinker, S. Turk, H. J. Rader, M. Barz, *Macromolecules* **2014**, *47*, 928-936.

[51] D. H. A. Correa, C. H. I. Ramos, *Afr. J. Biochem. Res.* **2009**, *3*, 164-173.

[52] J. M. McKim, *Combinatorial Chem. High Throughput Screening* **2010**, *13*, 188-206.

**The effect of two key architectural parameters of star-shaped SNAPPs (number of arms and arm length) on their biological activity, is examined**. It is found that SNAPPs bearing more and longer polypeptide arms display stronger antimicrobial effects, leading to the discovery of two more potent SNAPPs and new star SNAPP architectures which are easier to synthesize without losing significant biological activity.

**SNAPP, antimicrobial, star polymer, architecture, polypeptide**

Steven J. Shirbin, Ignacio Insua, James A. Holden, Jason C. Lenzo, Eric. C Reynolds, Neil M. O'Brien-Simpson and Greg G. Qiao

**Architectural Effects of Star-Shaped 'Structurally Nanoengineered Antimicrobial Peptide Polymers' (SNAPPs) on their Biological Activity**